Microstructure and Mechanical Properties of FSLA Steel Produced by the Binder Jet Process

Chris Schade, Tom Murphy, and Kerri Horvay
Hoeganaes Corporation
Cinnaminson, NJ 08077

ABSTRACT

An alloy, called FSLA (free-sintering low-alloy), was designed and implemented for use with binder jet printing. This work focuses on various heat treatments that can be utilized with the alloy to produce a range of properties for various applications. The microstructure of the alloy can be varied post-sintering, by heat treatment, to give a wide range of mechanical properties that are suitable for automotive components. The alloy constituents are formulated so that upon cooling from the sintering temperature, the transformation products allow the alloy to reach the required mechanical properties. The hardenability of the alloy is such that ultimate tensile strengths in excess of 1000 MPa can be obtained by inter-critically annealing the material and air cooling. Various heat treatments and their corresponding mechanical properties are reviewed.

INTRODUCTION

Metal Binder Jetting (MBJ) has garnered more interest as an additive manufacturing technique primarily due to the increased speed at which material can be printed and the wider range of materials that can be processed when compared to techniques like Laser Powder Bed Fusion (LPBF).[1-2] However, because of the low as printed density, the sintering process generally requires longer times and higher temperatures than conventional processes like metal injection molding (MIM). In addition, the binders utilized by the commercially available MBJ printers often interact with the powder surface, complicating the sintering process and requiring additional development efforts on the part of the end user. Physical attributes of the powder such as apparent density, tap density and flowability impact how the material interacts with the re-coater in the printer. For the most part, this has limited the availability of materials for MBJ to those which are developed with the printer itself, such as 316L stainless steel. As mentioned previously, the increase in printing speed of MBJ makes the process attractive for serial production of cost-sensitive parts, such as those used by the automotive industry. Due to the decoupling of shaping and solidification into a two-step process (printing/sintering), production throughput can be increased 10-50 times compared with other AM technologies e.g., LPBF. In addition, MBJ is not limited to alloys that are weldable, but can utilize a wider range of materials. To achieve high densities (>98% relative density), fine powders are used with a mean particle size, d_{50}, ranging from 10-15 µm. Utilizing fine powders results in a superior surface quality, about 20% better than LPBF.

Because of these benefits, the automotive industry in now more actively engaged in evaluating MBJ for production of automotive parts. In particular, because of the ability of 3D printing to

produce designs that are conducive to weight reductions, a particular interest of the automotive makers is the application of sheet material for body and chassis parts. The steels used for these applications are generally classified as Advanced High Strength Steels (AHSS).

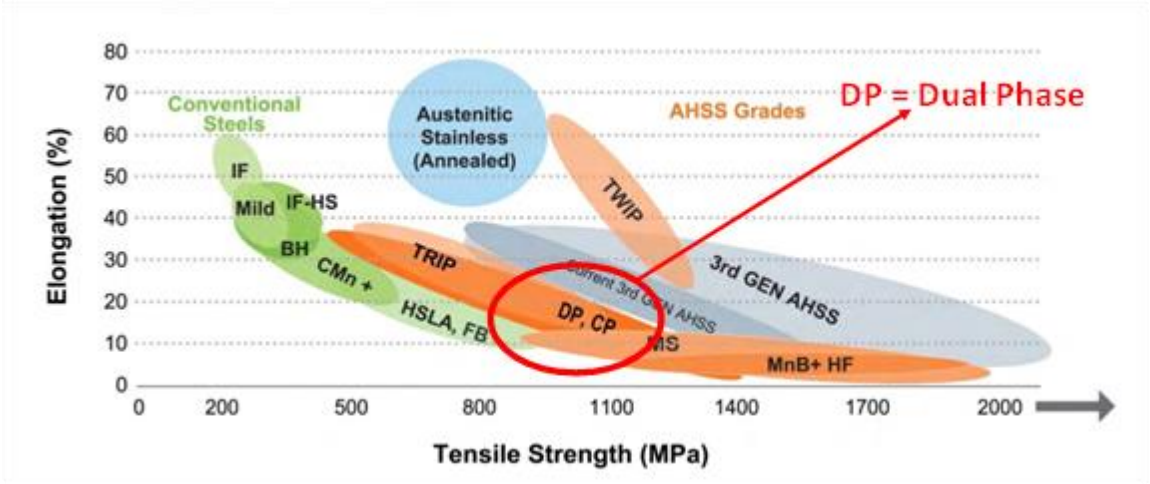

Figure 1: Steel Strength Ductility Diagram, illustrating the range of properties available from today's AHSS grades.[3]

Advanced high-strength steels, or micro-alloyed steels, generally give superior mechanical properties utilizing low levels of alloy content coupled with thermo-mechanical processing; typically rolling in combination with accelerated cooling (Figure 1). Dual-phase (DP) steels are considered a subclass of AHSS and exhibit a microstructure consisting of a hard phase (primarily martensite and/or bainite) in a matrix of ferrite. Due to their composite microstructures, dual-phase steels exhibit excellent mechanical properties with ultimate tensile strengths (UTS) generally dependent primarily on the volume fraction of martensite.[4-6] These steels are therefore classified according to their ultimate tensile strength; for example, DP500 has a UTS of approximately 500 MPa, while DP1000 would have an approximate UTS of 1000 MPa.

In a previous paper, an alloy called FSLA (Free Sintering Low Alloy) was introduced for MBJ which was comparable in properties to DP600 (i.e. UTS = 600 MPa).[7] Unlike other low alloy steels, the chemistry of the FSLA alloy was tailored to have a mixed microstructure of approximately 50 volume percent ferrite and 50 volume percent austenite at the sintering temperatures. Work by previous authors had suggested that the increase in grain boundary area between the austenite and ferrite would increase the diffusion and lead to higher sintered densities.[8-9] This was proven to be the case as the MBJ- FSLA had superior sintered density than other low alloy steels. The ferrite stabilizing elements (chromium, molybdenum and silicon) were all chosen because of their hardenability characteristics, which allowed for the transformation of the austenite to martensite at moderate cooling rates. The alloy chemical composition allowed for intercritically annealing in a two-phase region of austenite and ferrite. With appropriate cooling rate, the austenite will transform to martensite (and/or bainite) and a final microstructure of different levels of ferrite and martensite/bainite (the typical microstructure of dual phase steels) can be accomplished. In the previous work already cited, the main objective was to match the property values for DP600. These were obtained by

intercritically annealing the FSLA at 850 °C and cooling at a rate of 1.3 °C/sec. The properties and microstructure of the material processed in this way are shown in Figure 2.[7]

	UTS [MPa]	0.2%YS [MPa]	Elongation [%]	Hardness [HRA]
DP600 (Salzgitter)	580-670	330-470	24 (min)	---
Run 1	684	397	19.9	51
Run 2	691	383	19.4	49
Run 3	673	387	20.3	50
Run 4	692	404	19.9	52
Run 5	696	404	19.2	52
Run 6	683	396	19.4	51
Average	687	395	19.7	51

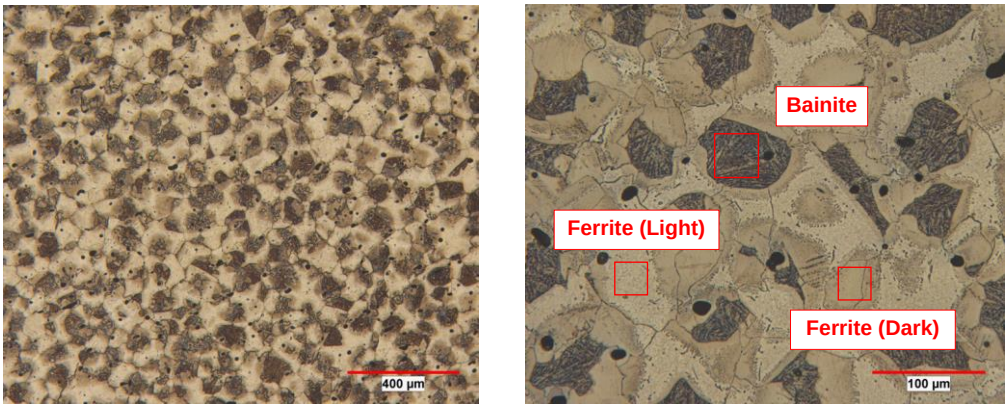

(a) **(b)**

Figure 2: Mechanical properties and microstructure of FSLA alloy intercritically annealed at 850 °C and cooled at a rate of 1.3 °C/s. (a) general microstructure and (b) higher magnification identifying the bainite as well as the two types of ferrite dislocated (dark) and non-dislocated.[7] Note: DP600 wrought properties were taken from Salzgitter shown in yellow on the table.[10]

The target properties of the wrought DP600 were consistently met by this development work as evident by the table in Figure 2, but the ability to heat treat the FSLA alloy in the two-phase region lends itself to further investigation into the achievable properties of this alloy. As mentioned in the introduction, an alloy processed to achieve a range of mechanical post-printing is desirable to save on printer development work. Therefore, this paper details additional heat treatment routines that can expand the range of ultimate tensile strength and ductility combinations of the FSLA alloy without changes to its composition or printing parameters.

EXPERIMENTAL PROCEDURE

Powders utilized in this study were air melted and gas atomized with nitrogen. Chemical analysis and powder properties are listed in Table I.

Table I: Powder properties of Air Melted- Gas Atomized FSLA. Chemical composition shown in weight percent.

	Apparent Density	Tap Density	Carbon	Sulfur	Oxygen	Nitrogen	d_{10}	d_{50}	d_{90}
Material	**g/cm^3**	**g/cm^3**	**wt.%**	**wt.%**	**wt.%**	**wt.%**	**Micrometers**	**Micrometers**	**Micrometers**
FSLA Powder	3.2	4.9	0.14	0.007	0.06	0.01	5.7	14.0	24.4

Material	Mn	Cr	Ni	Mo	Nb	V	Si
FSLA Powder	0.20	1.60	0.06	1.45	0.18	0.18	1.64

All test samples were printed on an HP Multi Jet Fusion Printer, with a water-based binder at a 50-micrometer layer thickness.[11]

Test pieces were sintered at DSH Technologies utilizing MIM3045T furnaces from Elnik Systems. These furnaces combine the thermal debind and the sinter process in one furnace. The equipment has a maximum temperature of 1600 ^oC with partial pressure or vacuum control. The furnace is an all-metal process zone with atmosphere capabilities of pure hydrogen, nitrogen, argon, or vacuum environments. For this study, the test pieces were sintered in a high temperature Elnik MIM at 1380 ^oC for 30 minutes in an atmosphere of 95 vol.% nitrogen / 5 vol.% hydrogen.

For continuous heat treatment, a high temperature Abbott continuous-belt furnace was used at indicated temperatures for 30 minutes in an atmosphere of 95 vol.% nitrogen / 5 vol.% hydrogen.

Prior to mechanical testing, green and sintered densities, dimensional change (DC), and apparent hardness were determined on the tensile and transverse rupture (TR) samples. Five tensile specimens (flat dogbones/unmachined) and five TR specimens were evaluated for each composition. The densities of the green and sintered steels were determined in accordance with MPIF Standard 42. Tensile testing followed MPIF Standard 10, and apparent hardness measurements were made on the tensile and TR specimens, in accordance with MPIF Standard 43. [12]

Porosity measurements were made on metallographically prepared cross-sections removed from entire test parts. A Clemex automated image analysis system was used to measure and map the porosity on as-prepared surfaces using a predetermined gray level to separate the dark void space and from the highly light reflective metallic regions. This provided the opportunity to estimate the pore content in both the sample volume and in localized regions.

Specimens for microstructural characterization were prepared using standard metallographic procedures. Subsequently, they were examined by optical microscopy in the polished and etched (2 vol.% nital / 4 wt.% picral) conditions.

In addition, the microstructure was revealed, and color was used to separate the transformation products with a two-step, etch/stain process. First, the microstructure was defined with a light pre-etch by immersing the sample in Vilella's Reagent (5 mL HCl + 1 g picric acid + 100 mL ethyl alcohol), rinsing with warm water, and drying with filtered compressed air. In the second step, the pre-etched sample was immersed in a freshly prepared solution of 10 g sodium metabisulphite ($Na_2S_2O_5$) in 100 mL deionized or distilled water, rinsed with warm water and alcohol, then dried with filtered compressed air.

The Electron Probe Micro-Analysis (EPMA) was conducted with the aid of JEOL JXA-8530F Field Emission Electron Probe Microanalyzer (EPMA) with JEOL XEDS & xCLent Cathodoluminescence, using a tungsten filament or a LaB6 tip at the University of Pittsburgh. Specimens for EPMA were prepared according to the standard preparation followed by vibro-polishing for 3 hours with 0.05 μm nanometer alumina suspension. The measurements were performed using 1000x and 1500x magnifications, at an accelerating voltage of 20 kV, a beam current of 100 nA, and a probe diameter of 1 μm.

RESULTS AND DISCUSSION

One of the unique features of the FSLA alloy is the wide range of temperatures in which the alloy can be heat treated in a two-phase region of austenite and ferrite. This is shown by the Calphad diagram in Figure 3. When heat treated at a temperature of approximately 870 ^{o}C, the microstructure of the FSLA alloy is > 90% ferrite. Conversely, when held at temperatures near 1150 ^{o}C, the microstructure is ~ 90% austenite which can transform to either bainite or martensite depending on the cooling rate. One of the key features of dual phase steels is the ability to vary the mechanical properties by changing the levels of martensite, bainite and ferrite. If a material of higher strength and hardness is required, intercritical annealing is performed at a temperature at which there is a high level of austenite that can transform during cooling. If a material with lower strength but better ductility is required, an intercritical anneal temperature which favors the formation of the softer ferrite phase is chosen. In order to evaluate the range of properties the FSLA alloy could exhibit, it was decided to test the extreme differences in the phases; an alloy that was ~ 90% ferrite and an alloy that was 90% transformation products martensite/bainite).

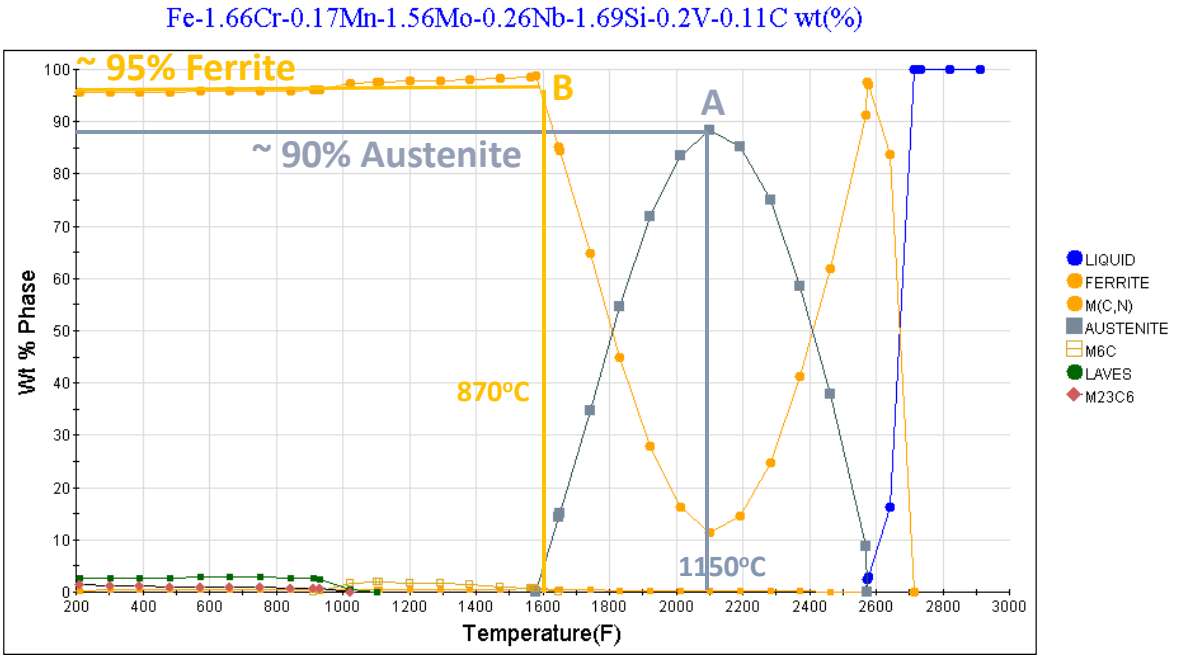

Figure 3: CALPHAD generated diagram for the phases present at various temperatures for the FSLA alloy chemical composition shown in Table I.

The first set of experiments involved heating the FSLA alloys to a temperature of around 1200 ^{o}C, which corresponds to point "A" on Figure 3. At this temperature, at equilibrium, the FSLA microstructure should consist of approximately 85% austenite, which can then transform to martensite/bainite depending on the cooling rate. It is important to note that the chromium, molybdenum and silicon levels in the alloy combine to give a high hardenability as this alloy can transform with only furnace cooling (no quenching). This is a distinct advantage of the alloy formulation as these alloying elements also allow for the proper phase balance at the sintering temperature to enhance diffusion by formation of austenite/ferrite phase boundaries.

However, the diagram in Figure 3 is an equilibrium diagram and does not account for the kinetics of the phase transformations to take place. The initial microstructure of the test specimens that exists after sintering and subsequent cooling from the sintering temperature is a mixture of transformation products (martensite/bainite) and ferrite. When the test specimens are heated to 1200 ^{o}C, both the transformation products and the ferrite need to change crystal structure to austenite. This is done by partitioning of elements and this takes time. In order to evaluate the amount of time needed to complete the transformations, sintered samples of the FSLA were heat treated for 1,2,3,4 and 5 hours at 1200 ^{o}C in a vacuum furnace under a partial pressure of nitrogen. Tensile properties and hardness values were measured after each of the time increments. Quantitative metallography was used to determine the level of martensite in the specimens. Figure 4 shows the results of the experiments. Between 1-3 hours, the martensite values fell far short of the predicted equilibrium values shown in Figure 3. After 3 hours the martensite volume fraction approached the 80% value predicted by the Calphad diagram. The ultimate tensile strength and hardness values reached a maximum at around 4-5 hours eventually achieving a UTS of 1050 MPa. It also should be noted that heat treating at various times leads to a variation on the amount of martensite which produces UTS strengths from 800 MPa in the as

sintered condition to 1050 MPa after 3-5 hours at 1200 °C. This flexibility in properties allows the same printed material to be used in a range of applications.

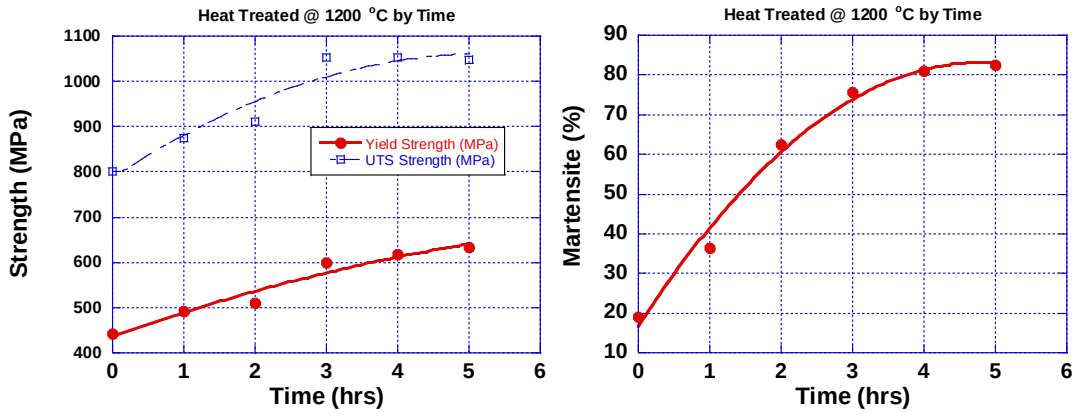

Figure 4: Effect of time at 1200°C on Ultimate Tensile Strength (UTS) and Yield Strength (YS) (left) and volume fraction of martensite formed (right).

The mechanism for the different levels of martensite formation is due to diffusion of the alloying elements, most notably carbon, chromium, silicon and molybdenum. Carbon, which diffuses interstitially, has the biggest impact since it has both, the greater mobility and also is the most effective element in hardening the martensite.[13-15] Figure 5 shows an EPMA result of a scan across both the ferrite and martensite grains in samples that were sintered for various times at 1200 °C. The graphs of the various elements show that carbon has the biggest variation between the ferrite and martensite grains, reaching a maximum at 1 hour with an amount almost double the value of the ferrite (0.09 wt% versus 0.045 wt%). In general, all elements seem to reach a value of equilibrium after three hours. Although the martensite should have its maximum hardness after 1 hour, the amount of martensite, as shown, increases and starts to level of after 3 hours. Therefore, the maximum strength in the alloy is a combination of partitioning of the carbon to the austenite at high 1200 °C and the amount of martensite that is formed upon cooling.

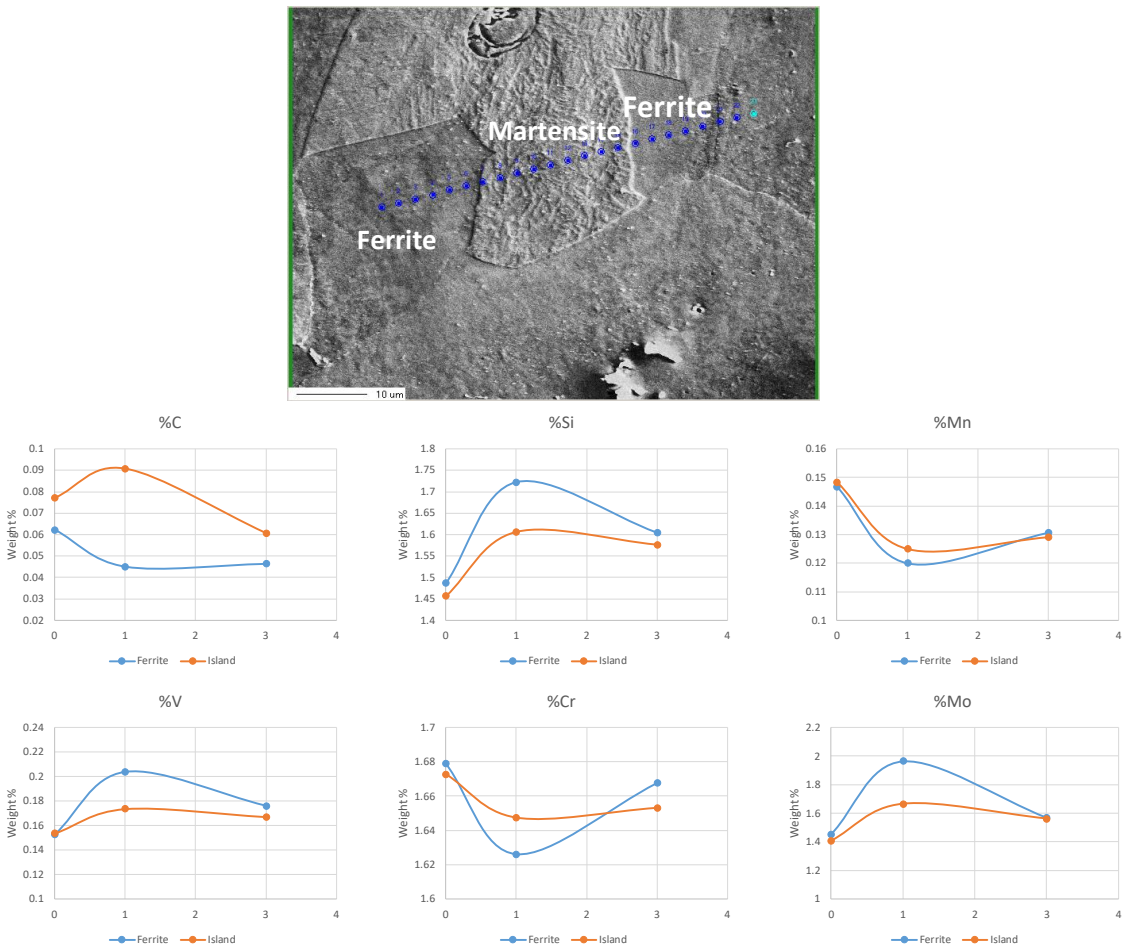

Figure 5: Example of Electron Probe Micro Analysis (EPMA) for various elements across ferrite and martensite islands of FSLA heat treated at 1200 ^{o}C for various time in hrs. (shown on the X axis).

Since the diffusion of carbon can take place with both time and temperature, different levels of carbon in the martensite can be achieved by intercritically annealing for different times and temperatures, thus increasing the variation in mechanical properties that can be achieved.

A second set of experiments were conducted in which the FSLA was intercritically annealed in a range of 800-900 ^{o}C. At this temperature, the indication from Figure 3 (Point B) is that the microstructure of the alloy will be predominantly ferrite which will allow for a material with a much higher level of ductility. This increase in ductility (elongation) is useful in the sheet metal components where the energy from impact needs to be absorbed (mainly the chassis area such as side-panels). The microstructure of the FSLA alloy after the sintering process is a mixture of ferrite and some transformation products (usually bainite). Therefore, it was necessary to re-austenitize the samples, allowing the already transformed ferrite (from sintering) to transform to austenite and allowing for a maximum amount of ferrite to be formed by holding at this temperature. For this reason, the samples were heated for 1 hour at 1200 ^{o}C to form all austenite, followed by a furnace cool to an intercritical anneal temperature in a range of 800 to 900 ^{o}C.

Holding at these temperatures allowed for the transformation of some of the high temperature austenite to ferrite. In order to maximize ductility, there is a necessity to balance the level of ferrite which predominates at the lower temperatures (800 ^{o}C) with the amount of carbide formation from elements like niobium, vanadium and molybdenum. The precipitates that form from these elements were useful in creating the high strength necessary in the DP980 type alloys, but hinder dislocation motion and therefore limit the ductility of the alloy at the range necessary to achieve the desired elongation values for alloys such as DP480 (UTS = 480 MPa).

To optimize the mechanical properties, three intercritical anneal temperatures were used: 825, 871 and 898 ^{o}C. The amount of ferrite was measured in specimens for all three temperatures as shown in Figure 6. At the lower temperatures (825 ^{o}C), the amount of ferrite was maximized at 92%. However, the number of carbides were increased. Conversely, at 898 ^{o}C, the carbides were minimized but the level of ferrite was reduced to 71%. Since ferrite dominates the ductility of the alloy it was decided to focus on intercritically annealing at the lower temperatures, trying to minimize the impact of the carbides on the strength.

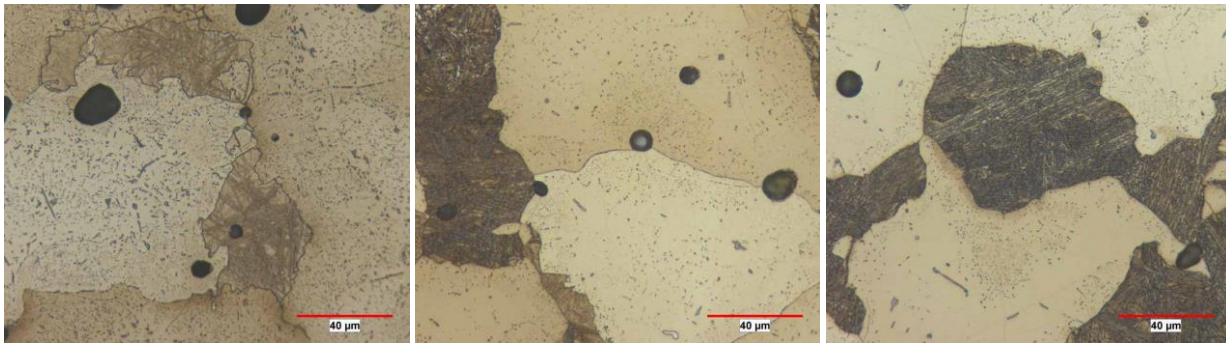

Figure 6: Optical micrographs of the FSLA alloy heat treated at 1200 ^{o}C for 1 hour then furnace cooled and held at 825,871 and 898 ^{o}C for 2 hours to maximize the ferrite content. Note: as ferrite content decreases at the higher temperatures, the volume of carbides also decreases.

Having already established that the maximum amount of ferrite that could be produced with intercritical anneal temperatures of around 800 ^{o}C, it was necessary to limit the impact of the carbides on increasing the tensile strength and reducing ductility. Based on thermodynamics the formation of the carbides is inevitable, however limiting the size and frequency of the carbides was investigated in order to reach the target properties of a DP480 material. One obvious way to limit the carbide formation is to restrict the amount of carbon available to combine with the carbide-forming elements such as chromium, silicon, molybdenum, vanadium and niobium. A method for reducing the carbon available is to make sure that the carbon content associated with the martensite is as high as possible. Therefore, the variation of carbon in both the ferrite and the martensite was studied as a function of the time and temperature for the intercritical anneal.

EPMA measurements were taken across the martensite grains in samples annealed at 800 ºC for time intervals of 10 secs, 30, 60 and 120 mins. The sample isothermally held at 10 seconds was meant as a baseline measurement for the starting carbon. An example of a microprobe measurement is shown in Figure 7. Here, the carbon can be seen to be lower in the ferrite and increases as the microprobe crosses the ferrite/martensite interface with a maximum value achieved in the martensite grain. measurements of carbon content versus hold time at 800 ºC reveals that carbon increases from 0.087% at a hold time of 10 secs to a value of 0.102% at a hold time of 2 hours (increase of 15%). The hold time at 10 secs was just to ensure homogenization at the start of the measurements.

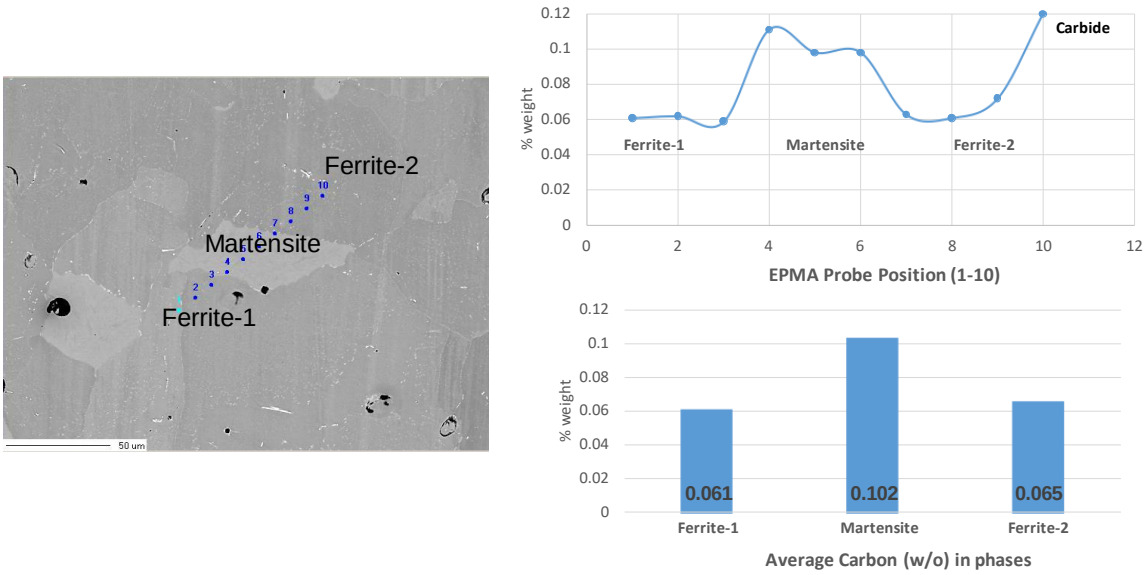

Fig. 7: EPMA measurements of carbon through ferrite and martensite grains and average carbon level in each grain measured.

Since the level of carbon in the martensite is higher, there is less available to strengthen the ferrite, and since the ferrite is the dominant matrix phase, the ductility of the alloy is expected to increase. In addition, if the carbon is increased in the martensite, less carbon is available to form carbides. In order to examine the impact of various times at temperatures on carbide formation, the amount and size of carbides was determined from quantitative measurements. Figure 8 shows scanning electron microscope (SEM) images of samples isothermally held at 30 mins, 60 mins and 120 mins at 800 ºC. As the isothermal hold time increased, there was only a slight increase in volume fraction of precipitates from 2.1 at 60 mins versus to 3.2% at 120 mins. The objective was to limit the growth of precipitates (carbides) that would strengthen the material and lower elongation; therefore 120 mins (2 hours) was chosen as the maximum heat treat time at 800 ºC. The average size of the precipitates did not increase significantly with the various hold times. It appears from the SEM images that the pre-existing precipitates coarsened while new precipitates started to form at 800 ºC. These two effects counter balanced each other, leading to very little

strength change but an increase in ductility because of the increased amount of ferrite allowing the properties to match the wrought material very closely.

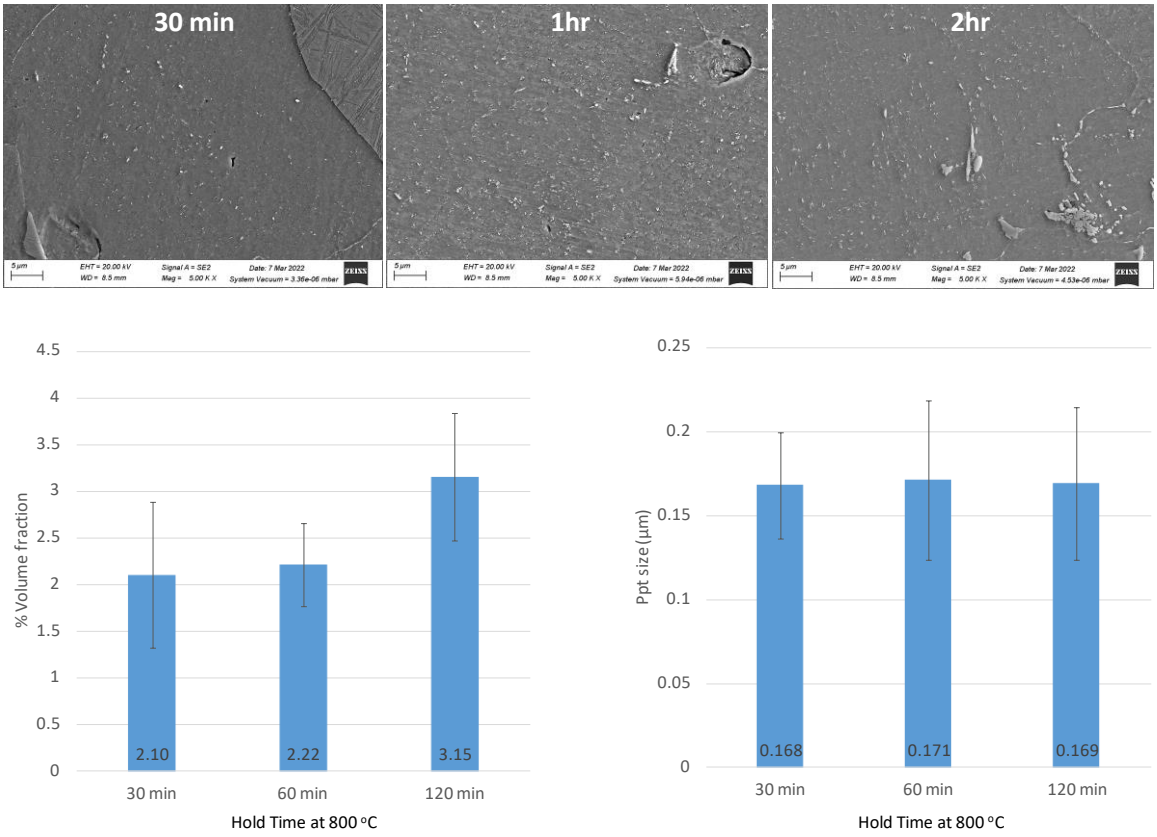

Figure 8: Volume fraction of precipitates (left) and precipitates size (right) as a function of hold time at 800 ^{o}C corresponding to SEM images (top).

Based on all results of the metallographic analysis, tensile properties were measured on the materials heat treated in the fashion described above. Table II shows the tensile properties for the FSLA austenitized at 1200 ^{o}C then furnace cooled to 800 ^{o}C and held for 2 hours. Considering the high strength of the alloy (UTS = 604 MPa) and the fact that the material produced from MBJ reaches only a density of approximately 97.5% of theoretical, the elongation value of 23% is very close to the wrought values requiring 24% minimum elongation.

Table II: Tensile properties of FSLA Austenitized at 1200 ^{o}C for 1 hour then furnace cooled to 800 ^{o}C for 2 hours then furnace cooled to room temperature.

Condition	UTS (MPa)	YS (MPa)	Elongation (%)	Apparent Hardness
1200^{o}C 1hr-800^{o}C 2hr	604	326	23	49 HRA

SUMMARY AND CONCLUSIONS

It is apparent from this discussion that the FSLA alloy properties can be varied significantly by the manner in which the material is heat treated after sintering. The alloys were initially developed as a replacement for a wrought DP600, which acquires its dual phase structure and mechanical properties through a combination of controlled rolling and intercritical anneal heat treatments. But in addition to the DP600, there are a range of DP alloys used in conventional wrought processing that have a range of ultimate tensile strengths ranging from 480 MPa to 1050 MPa.[16] In many cases, this is accomplished by increasing the carbon level to the same base alloy chemistry. However, in the FSLA alloy, the wide range of microstructures (transformation products and ferrite) that can be achieved by changing the intercritical annealing temperature along with the variation of the amount and size of the carbides leads to a very flexible alloy in terms of mechanical properties. This is highlighted in Figure 9 where elongation versus ultimate tensile strength for both the wrought versions of dual-phase alloys (DP450, D490, DP590, DP780 and DP980) and the FSLA alloy produced by MBJ are plotted. In the FSLA alloy, only the heat treatment is adjusted to tailor the mechanical properties so that development of print parameters is limited to one material, therefore, saving a significant amount of development time. Figure 9 shows the wide range of possible material properties for the FSLA.

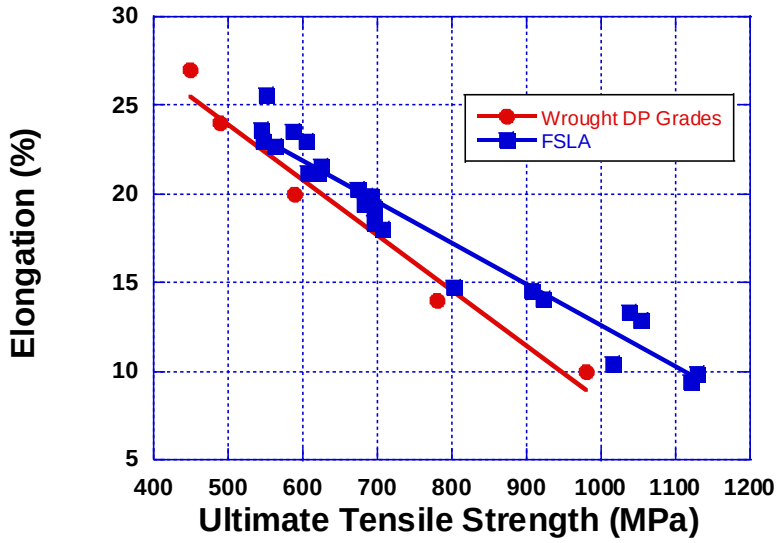

Figure 9: Mechanical properties of MBJ- FSLA compared with wrought versions of DP steels (DP450, D490, DP590, DP780 and DP980). [16]

New technologies like MBJ require tailored materials to fully utilize their production potential. The FSLA material is designed and intensively tested for binder jetting at GKN. It is shown that FSLA shows good printability and sinterability. A robust process route is developed to produce components with densities above 98%. Further improvement is ongoing at GKN. Particularly interesting is the wide range of material properties that can be achieved with one material without changing the printing and sintering processes. Within this study, heat treatment is

identified as a critical additional post-processing step. The FSLA material properties can meet different requirements and can be modified for different applications.

REFERENCES

1. W.E. Frazier, "Metal Additive Manufacturing: A Review", Journal of Material Engineering, Performance, 2014 Vol. 23, No.6 pp.1917-1928.
2. M. Li, W. Du, A. Elwany, Z. Pei, and C. Ma, "Metal Binder Jet Additive Manufacturing", Journal of Manufacturing Science and Engineering, Sept 2020, Vol. 142 No.9.
3. World Steel Auto: http:\\www.worldautosteel.org/
4. M.K. Singh, Application of Steel in Automotive Industry, Int. J. Emergin Technol. Adv. Eng. 6 (2016) 246–253.
5. C.C. Tasan, M. Diehl, D. Yan, M. Bechtold, F. Roters, L. Schemmann, C. Zheng, N. Peranio, D. Ponge, M. Koyama, K. Tsuzaki, D. Raabe, An Overview of Dual-Phase Steels: Advances in Microstructure-Oriented Processing and Micromechanically Guided Design, Annu. Rev. Mater. Res. 45 (2015) 391–431.
6. R.A. Kot and B.L. Bramfit, Editors, "Fundamentals of Dual Phase Steel," The Metallurgical Society of AIME, 1981.
7. C. Schade, T. Murphy, K. Horvay, A. Lawley and R. Doherty, Development of a Free Sintering Low Alloy (FSLA) Steel for the Binder jet Process, *Advances in Additive Manufacturing with Powder Metallurgy – 2021*, compiled by S. Atre and S. Jackson, Metal Powder Industries Federation, Princeton, NJ, 2021, part 7 pp.287-306.
8. N.B. Shaw and R.W.K. Honeycombe, "Some Factors Influencing the Sintering Behaviour of Austenitic Stainless Steels," Powder Metallurgy, 1977; vol. 20: pp. 191-198.
9. R.I. Sands and J.F. Watkinson, "Sintered Stainless Steels I.- The influence of Alloy Composition upon Compacting and Sintering Behaviour," Powder Metallurgy, 1960, No. 5, pp.85-104.
10. DP600 Product Datasheet from Salzgitter Flachstahl, Edition 07/10 page 1.
11. HP. Inc. Technical White Paper, "HP Metal Jet Technology," 2018, www8.hp.com/h20195/v2/GetPDF.aspx
12. *Standard Test Methods for Metals Powders and Powder Metallurgy Products*, Metal Powders Industry Federation, Princeton, NJ,2019.
13. M.C. Chatur Vedi and A.K. Jena, "Effect of Intercritical Annealing Temperature on Equilibrium between Ferrite and Austenite," Materials Science and Engineering, 94 1987, pp.L1-L3
14. G.R. Speich, "Physical Metallurgy of Dual Phase Steels," *Fundamentals of Dual Phase Steels*, The Metallurgical Society of AIME, R.A. Kot and B.L. Bramfit, Editors, pp.3-45.
15. P. Messein, J.C. Herman, and T. Greday, "Phase Transformation and Microstructures of Intercritically Annealed Dual Phase Steels," *Fundamentals of Dual Phase Steels*, The Metallurgical Society of AIME, R.A. Kot and B.L. Bramfit, Editors, pp.161-180.
16. Voest Alpine Product Data Sheet for Dual Phase Steels, June 2019, page 3. https://www.voestalpine.com/stahl/en/content/